Available online at www.sciencedirect.com
ScienceDirect
C. R. Physique 7 (2006) 573–583
COMPTES RENDUS PHYSIQUE
http://france.elsevier.com/direct/COMREN/

Turbulent transport in fusion magnetised plasmas/Transport turbulent dans les plasmas magnétisés de fusion

Introduction to turbulent transport in fusion plasmas

Xavier Garbet

Association Euratom-CEA, CEA/DSM/DRFC CEA-Cadarache, 13108 Saint Paul Lez Durance, France

Available online 9 August 2006

Abstract

This introduction presents the main instabilities responsible for turbulence in tokamak plasmas, and the prominent features of the resulting transport. The usual techniques to construct reduced transport models are described. These models can be tested by analysing steady state and transient regimes. Another way to test the theory is to use a similarity principle, similar to the one used in fluid mechanics. Finally, the physics involved in the formation and sustainment of transport barriers is presented. ***To cite this article: X. Garbet, C. R. Physique 7 (2006).***

Résumé

Introduction au transport turbulent dans les plasmas de fusion. Cette introduction présente les principales instabilités à l'origine de la turbulence dans les plasmas de tokamak, ainsi que les principales caractéristiques du transport turbulent qui en résulte. Les techniques usuelles permettant de construire un modèle de transport y sont décrites. Ces modèles peuvent être testés en analysant des régimes stationnaires et transitoires. Une autre façon de tester la théorie est d'utiliser un principe de similitude analogue à celui utilisé en mécanique des fluides. Finalement, les mécanismes physiques conduisant à la formation et l'entretien des barrières de transport sont décrits et commentés. ***Pour citer cet article : X. Garbet, C. R. Physique 7 (2006).***

Keywords: Fusion plasmas; Plasma turbulence

Mots-clés : Plasmas de fusion ; Turbulence dans les plasmas

1. Introduction

Understanding turbulent transport in magnetised plasmas is a subject of utmost importance for comprehending and optimising experiments in the present fusion devices, and also for designing future reactors. This appears as a fact when looking at the condition for obtaining a fusion power that is larger than the losses, the Lawson criterion, which states that the triple product $nT\tau_E$ (n is the density, T the temperature, τ_E the confinement time) must be larger than a critical value of the order of $3 \times 10^{21}\ \mathrm{m^{-3}\,keV\,s^{-1}}$. It turns out that the confinement time τ_E, which is basically a thermal relaxation time, is mainly determined by conductive losses, and therefore by turbulent transport. A vigorous and coordinated effort has been undertaken worldwide to improve our knowledge in this domain. This article is an introduction to this subject.

E-mail address: xavier.garbet@cea.fr (X. Garbet).

1631-0705/$ – see front matter
doi:10.1016/j.crhy.2006.06.002

The main instabilities that underlie turbulent transport in fusion plasmas are now well identified. However, the resulting turbulent transport remains hard to compute with adequate accuracy. The methodology for addressing this problem relies on an assumption of space and time scale separation between equilibrium and fluctuations. This assumption is the justification for developing a mean field theory of transport. A common recipe for building most models of transport is based on a quasi-linear theory, combined with a mixing-length rule. Transport models are usually tested by comparing the predicted profiles to experimental data. An alternative powerful technique consists of analysing transients, in particular heat modulation experiments. Turbulent transport can also be studied by using a similarity principle, analogous to that used in fluid mechanics. Dedicated experiments have led to dimensionless scaling laws, which give an insight into the nature of the turbulence.

An important issue for fusion plasmas is to reach situations where the turbulent transport is low, i.e., with an improved confinement. Transport barriers, which are regions where turbulence is reduced or quenched, are now routinely produced and maintained in tokamaks. Flow shear and/or magnetic shear play a central role in the formation and sustainment of these transport barriers. These regimes are usually reached above a critical value of the heating power, which should be minimized.

Several observations suggest that a mean field theory may not be appropriate for describing turbulent transport in tokamaks. Hence turbulence in magnetised plasmas has been intensively studied during recent years. Numerical simulations have made tremendous progress, and have addressed issues such as intermittency, turbulence self-organisation, structure dynamics and non diffusive transport. Diagnostics have been developed to measure fluctuations in tokamak plasmas with increasing spatial and time resolution. Also small size devices dedicated to turbulence studies have been built to elucidate the mechanisms that rule turbulence. Finally techniques have been developed to control turbulence, and have already given promising results.

This article is not intended to be an exhaustive overview of all these topics, but rather an introduction that should encourage the reader to explore the more extensive reviews presented in this special issue (references in section headlines point toward the other overviews of this special issue). The remainder of this paper is organised as follows. Section 2 briefly presents some general features and properties of turbulence in core tokamak plasmas. Transport models, similarity principle and analysis of transport are addressed in Section 3. The physics of transport barriers is studied in Section 4. Turbulence self-organisation and measurements are briefly presented in Sections 5 and 6. A conclusion follows.

2. A brief survey of micro-stability in tokamak plasmas

2.1. A brief description of the geometry and plasma equilibrium

This introduction is restricted to magnetic configurations of the tokamak type. Other configurations (stellarators, reversed field pinches, ...) present similarities, but also significant differences, whose description is beyond the scope of this introduction. The magnetic field in a tokamak has toroidal and poloidal components. Field lines are helical and are winded on torii, called magnetic surfaces. These magnetic surfaces are nested around a magnetic axis (see Fig. 1).

Each magnetic surface is labelled by an effective radius r, usually defined as the square root of the flux of toroidal magnetic field normalized to a reference magnetic field. The set of coordinates is completed by toroidal and poloidal angles φ and θ. The poloidal angle can be chosen such that the winding number q of the field lines, called safety factor, is constant on each magnetic surface, i.e., depends on r only (a mathematical definition of the winding number is $q(r) = \boldsymbol{B} \cdot \nabla\varphi / \boldsymbol{B} \cdot \nabla\theta$, where $\boldsymbol{B}$ is the equilibrium magnetic field). At the very edge of the plasma, field lines are intercepted by plasma facing components, i.e., are open. The magnetic surface separating the region where field lines are closed from the region where they are open is called separatrix. Also the modulus of the magnetic field decreases with the major radius. This is an important feature of the magnetic field topology. As a consequence, charged particles with low parallel velocities exhibit a bouncing trajectory in the minimum of the field. These particles are called trapped particles and play an important role in the instabilities that underlie turbulence. This role is weakened by collisions.

The description of transport in tokamaks usually makes use of time and spatial scale separation. Mean fields are the density, velocity and pressure (or temperature), averaged over fast time and spatial scales (in practice over poloidal and toroidal angles). These quantities, called equilibrium profiles, depend only on the radius and evolve on time scales much longer than a typical turbulence correlation time ($\sim$10 μs). Hence this averaging procedure allows writing transport equations in the radial direction (1D mean field theory). Fig. 2 shows schematic examples of

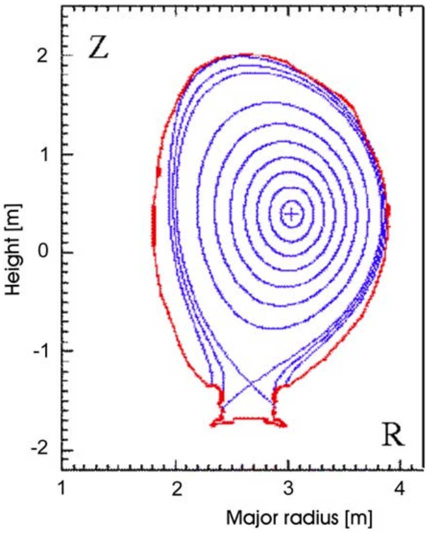

Fig. 1. Set of nested magnetic surfaces in a poloidal plane of the JET tokamak. The configuration is axisymmetric around the vertical axis (toroidal direction).

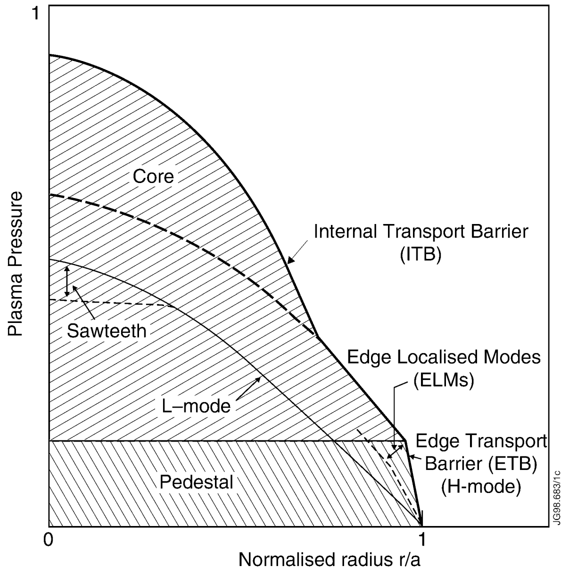

Fig. 2. Schematic pressure profiles in a tokamak. Standard conditions correspond to 'L-mode' plasmas. Transport barriers may develop in the edge ('H-mode'), and/or in the core (Internal Transport Barriers, ITBs).

pressure profiles. Transport barriers develop in tokamak plasmas when appropriate conditions are met (usually when the heating power exceeds a critical value). A transport barrier will be defined here as a region where turbulence is strongly reduced, ideally quenched. The result is a steepening of the profiles, as can be easily verified from the Fourier law relating the heat flux to the temperature gradient: at constant flux, a decrease of the thermal conductivity leads to an increase of the temperature gradient. Two situations occur in tokamaks: edge transport barriers (originally called H-mode for 'High' confinement) and internal transport barriers (ITBs) (see Fig. 2 for typical shapes of profiles in this case).

2.2. *Micro-instabilities*

The whole spectrum of instabilities in tokamaks is quite rich. Most micro-instabilities belong, in essence, to the family of interchange modes. An interchange mode is unstable when the gradient of magnetic field is aligned with the gradient of equilibrium pressure. In this case the exchange of two flux tubes around a field line releases free energy. Such a situation occurs in a tokamak on the 'low field side' (the modulus of the magnetic field decreases with the major radius in a tokamak). Conversely the plasma is locally stable with respect to interchange on the 'high field side'. Also trapped particles are localised on the low field side, as this corresponds to the zone of minimum field along the field lines. Hence trapped particles are expected to play a prominent role in the interchange process. Last, but not the least, field lines connect locally stable and unstable regions. This process leads to modes which tend to be aligned along the equilibrium magnetic field. In other words, the typical transverse size ($\sim 10^{-2}$ m) of a mode is much smaller than its wavelength along the magnetic field (~ 10 m). This feature persists in the non linear regime. Hence turbulence in tokamak plasmas is quasi-2D. 3D effects cannot be ignored though, as the direction of the magnetic field changes spatially (magnetic shear). The detailed stability analysis is beyond the scope of this introduction and only the most prominent features will be presented here.

For the sake of simplicity, we will restrict this survey to the main low wave number electrostatic micro-instabilities in core plasmas: Ion Temperature Gradient (ITG) driven modes and Trapped Electron Modes (TEM) [1,2] (called here ion and electron modes for simplicity). Electrostatic means here that perturbations of the magnetic field are ignored, so that only the perturbed electric field matters. This assumption is appropriate if the plasma beta $\beta = 2\mu_0 p/B^2$ (p is the total pressure, and B the magnetic field) is lower than the instability threshold for electromagnetic interchange modes (called 'kinetic ballooning modes') [3]. This simplification is actually questionable in the edge of tokamaks,

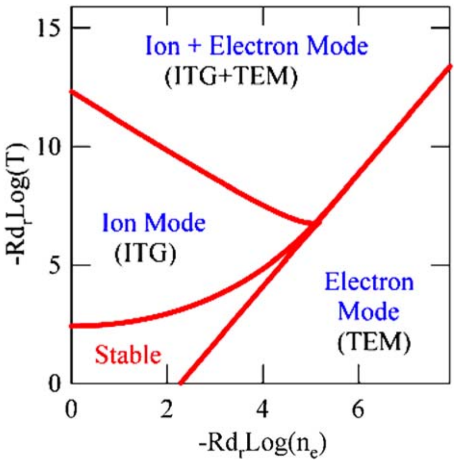

Fig. 3. Stability diagram of ITG/TEM modes. Electron and ion temperatures are equal.

where electromagnetic effects are known to be important. Also the electron temperature profile is supposed to be stable with respect to small scale electron temperature gradient driven modes [4]. However, it must be kept in mind that these modes may contribute significantly to electron transport for dominant electron heating.

ITG/TEM modes are unstable in the limit of large wavelengths such that $k_\perp \rho_i < 1$, where $k_\perp$ is the perpendicular wave number and ρ_i is the ion Larmor radius ($\rho_i = (m_i T_i)^{1/2}/e_i B$ where m_i is the ion mass, and T_i is the ion temperature, e_i the ion charge). In the non-linear regime, they produce particle, momentum, electron and ion heat transport. An important property of these micro-modes is the existence of an instability threshold. For a given profile of safety factor, the threshold of a pure ion mode (i.e., when the electron response follow a Bolzmann law) appears as a critical ion temperature logarithmic gradient $-R\nabla T_i/T_i$ (R is the major radius) that depends on the logarithmic density gradient $-R\nabla n_i/n_i$, and on the ratio of electron to ion temperature T_e/T_i. An ion mode usually rotates in the ion diamagnetic direction (the ion diamagnetic velocity is $\boldsymbol{V}^*_{p_i} = \boldsymbol{B} \times \nabla p_i/n_i e_i B^2$, where p_i is the ion pressure, n_i the ion density). Trapped electron modes usually rotate in the electron diamagnetic direction and are mainly driven through a resonant interaction of the modes with trapped electrons at the precession frequency. The threshold is a critical value of $-R\nabla T_e/T_e$ that depends on $-R\nabla n_e/n_e$ and the fraction of trapped electrons f_t. A separate treatment of ion and electron modes is usually an oversimplification. Nevertheless, there exists experimental situations where one branch is dominant, for instance when one species is hotter than the other.

Fig. 3 shows an example of stability diagram in the special case where electron and ion temperatures are equal, $T_e = T_i$. Depending on the values of gradient lengths, 0, 1 or 2 modes may be unstable. Well above all thresholds, both branches combine and the growth rate exhibits the typical expression for an interchange mode

$$\gamma_0^2 = f_t \omega_{de} \omega^*_{pe} + \omega_{di} \omega^*_{pi} \tag{1}$$

where $\omega^*_{ps} = k_\theta V^*_{ps}$ and $\omega_{ds} = 2k_\theta \lambda_s V_{ds}$($V_{ds}$ is the drift velocity due to the magnetic field curvature, $V_{ds} = -2T_s/e_s BR$, k_θ a poloidal wave number and $\boldsymbol{V}^*_{p_s} = \boldsymbol{B} \times \nabla p_s/n_s e_s B^2$ is called the diamagnetic velocity of the species 's'). The parameter λ_s depends on the magnetic shear $s = \mathrm{d}\,\mathrm{Log}(q)/\mathrm{d}\,\mathrm{Log}(r)$. More precisely, $\lambda_e = 1/4 + 2s/3$ for trapped electrons and $\lambda_i = \langle \cos(\theta) + s\theta \sin(\theta) \rangle$ for ions, where the bracket indicates an average over the mode poloidal structure. There also exists a branch of ITG modes, which does not belong to the interchange family (slab ITG modes). The growth rate of slab ITG modes exhibits a scaling comparable to Eq. (1), but the amplitude is smaller.

2.3. Turbulence simulations [5]

Turbulence has long been computed by using fluid equations. For a strong and homogeneous magnetic field, the fluid equations are very close to those describing a 2D incompressible rotating fluid, where the electric potential plays the same role as the stream function, and the magnetic field replaces the rotation angular frequency. Starting from this idealised situation, several ingredients have been added progressively since the early 1980s: simulations are now

3D, describe several species including impurities, fluctuations are electromagnetic, and the full toroidal geometry is implemented. The status of 3D simulations can now be considered as satisfactory, although still progressing, in particular to avoid a separation between equilibrium and fluctuating quantities.

However, while plasmas are getting closer to the conditions for achieving fusion, they are less and less collisional since the collision frequency decreases with increasing temperature. In weakly collisional plasmas, charged particles experience resonant interactions with the electromagnetic field. These resonant processes cannot be described correctly by fluid equations. Hence the distribution function of each species must be computed by solving a kinetic (Vlasov) equation, coupled to Maxwell equations via charge and current densities. This means in principle solving a 6D problem (3 directions for space and 3 for velocities). In practice, the cyclotron motion of particles is much faster than the dynamics of turbulent structures. This allows averaging the equations over the fast cyclotron motion. A Vlasov equation can be written for the average distribution function. The new problem is now 4D (typically 3 coordinates for the guiding-centre, which is the centre of the cyclotron motion, and the parallel velocity), parameterised by a motion invariant (adiabatic invariant). This average Vlasov equation is called a gyrokinetic equation. Solving a 5D gyrokinetic equation for each species coupled to Maxwell equations is a very difficult problem due to the large range of scales that must be simulated. Nevertheless gyrokinetic simulations are now routinely run thanks to the progress made in the domains of supercomputers and numerical techniques.

3. Transport models

3.1. Building a transport model [6] and testing it [7]

Many transport models are built on the basis of linear stability considerations. They provide quantitative fluxes following two separate steps. The first one is based on a quasi-linear expression of fluxes. Considering for instance the particle flux $\Gamma_e = \langle n_e v_{Er} \rangle$, where $\boldsymbol{v}_E = \boldsymbol{B} \times \nabla\phi / B^2$ is the $E \times B$ drift velocity (this is called 'electrostatic' turbulence). The particle flux can be expressed in Fourier space as

$$\Gamma_e = \sum_{\boldsymbol{k}\omega} n_{e,\boldsymbol{k}\omega} \frac{\mathrm{i}k_\theta \phi^*_{\boldsymbol{k}\omega}}{B} \tag{2}$$

where $\phi_{\boldsymbol{k}\omega}$ and $n_{\boldsymbol{k}\omega}$ are Fourier components of perturbed electric potential and density.

The quasi-linear expression consists in replacing the Fourier component of the density by its linear expression calculated with linearised fluid or kinetic equations. Assuming a convection equation $\partial_t n_e + \nabla \cdot (n_e \boldsymbol{v}_E) = 0$ and a uniform magnetic field (implying incompressibility $\nabla \cdot \boldsymbol{v}_E = 0$), the recipe given above yields a diffusive law $\Gamma_e = -D_{ql}\, \mathrm{d}n_e/\mathrm{d}r$. The quasi-linear diffusion coefficient D_{ql} is given by the expression

$$D_{ql} = \sum_{\boldsymbol{k}\omega} \left| \frac{k_\theta \phi_{\boldsymbol{k}\omega}}{B} \right|^2 \tau_{ck} \tag{3}$$

where τ_{ck} is a correlation time as scale $1/k$, and the summation index runs over poloidal and toroidal wave numbers. This expression can be understood as a random walk estimate for a fluctuating velocity $v_{E,k\omega} = -\mathrm{i}k_\theta \phi_{k\omega}/B$ (see Fig. 4).

A similar exercise can be carried out for electron and ion heat fluxes, $\phi_{Ee} = 3/2\langle p_e v_{Er} \rangle$ and $\phi_{Ei} = 3/2\langle p_i v_{Er} \rangle$, respectively, leading to a thermal diffusivity $\chi_{e,i} = 3/2 D_{ql}$. In fact an advection equation is oversimplified, and the whole set of fluid or kinetic linearised equations must be kept when calculating the quasi-linear fluxes. Eq. (3) depends on the level of potential fluctuations, which is unknown at this stage.

The second step consists of using a mixing-length rule to determine the level of fluctuations. The simplest version of this rule yields the level of fluctuation $e\phi_k/T_e = 1/k_\perp L_p$ (L_p is a pressure gradient length—here ϕ_k is an r.m.s. level averaged over time). This approximation is certainly the weakest part of the derivation of any transport model. For instance one would expect the level of fluctuation to vanish at the instability threshold. Various improvements have been proposed to account for these effects. A minimal improvement is to use an estimate that increases with the growth rate, i.e.,

$$\frac{e\phi_{k\omega}}{T_e} = \frac{\gamma_k}{\omega_p^*} \frac{1}{k_\perp L_p} \tag{4}$$

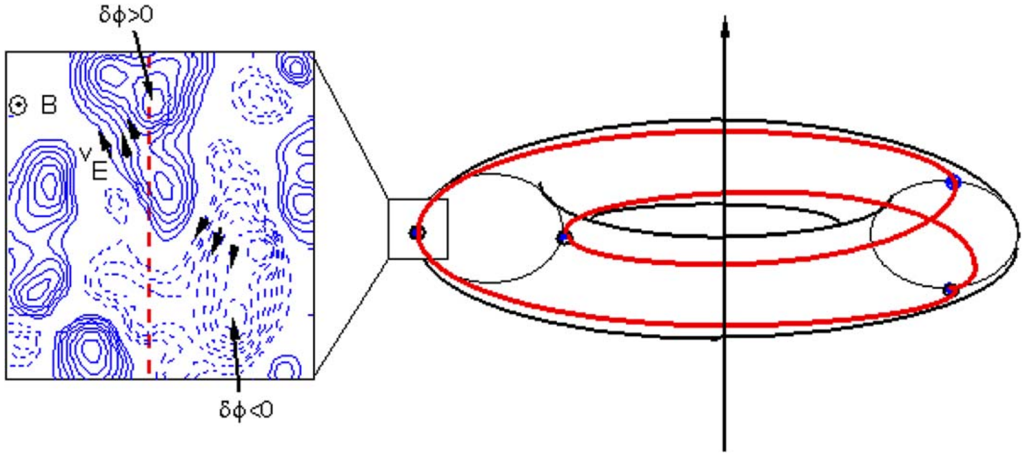

Fig. 4. Random walk experienced by a charged particle in an electrostatic turbulence. The center of the cyclotron motion ('guiding center') approximately follows a field line (line in bold). The transverse velocity of the guiding center (mainly the electric drift velocity $\boldsymbol{v}_E = \boldsymbol{B} \times \nabla\phi/B^2$) fluctuates due to perturbations of the electric potential ϕ (contour lines of ϕ are shown in the box, a set of closed lines is called a 'vortex', 'eddy' or 'convective cell'). This process leads to a diffusion and a transport coefficient of the order of $\langle|\boldsymbol{v}_E|^2\rangle\tau_c$, where τ_c is a typical correlation time.

where γ_k is the linear growth rate at scale $1/k$ and ω_p^* the diamagnetic frequency. This expression, combined with the above quasi-linear estimate, and $\tau_{ck} \propto 1/\gamma_k$ yields the mixing-length diffusion coefficient

$$D_{ml} = \sum_k \frac{\gamma_k}{k_\perp^2} \tag{5}$$

The Weiland [8] and GLF23 [9] models provide values of the linear growth rates γ_k. However they are based on fluid equations, which often predict values for the threshold that are too low. In fact the GLF23 model uses modified fluid equations to correct this drawback. Still the most accurate procedure to the calculate growth rates is to solve a kinetic equation to determine the plasma response [10,11]. The Weiland, GLF23, and mixed Bohm–gyroBohm [12] models are the most widely used.

An alternative picture emerges in the particular case where turbulent transport becomes very large when gradients cross the stability threshold. In this case, the profiles stay marginally stable, i.e., gradients are stuck to their critical value. This is called 'profile stiffness' [13]. In practice, only part of the profile is close to marginal stability. This concept is helpful to interpret experiments, when combined with linear stability analysis. An intermediate approach in between predictive transport modelling and strong profile stiffness consists of using a semi-empirical critical gradient model [14]. Assuming a gyroBohm scaling and electrostatic turbulence (see next section), a critical gradient model is of the form (for each species)

$$\chi_{\mathrm{cgm}} = \chi_{gB}\left[\chi_s\left(\frac{-R\partial_r T}{T} - \kappa_c\right) H\left(\frac{-R\partial_r T}{T} - \kappa_c\right) + \chi_0\right] \tag{6}$$

where $\chi_{gB} = q^\nu (T/eB)\rho_s/R$. Here χ_s is a number that characterises the stiffness, κ_c, is the instability threshold, and $H(x)$ is a Heaviside function. Strong stiffness corresponds to a large value of χ_s. It is also assumed that a finite diffusivity persists when the gradient is below the threshold, with an amplitude χ_0. The safety factor q accounts for the improvement of confinement with plasma current. The value $\nu = 3/2$ is presently the best compromise between various experiments. Hence a critical gradient model is characterised by 3 parameters only and is often used as a first analysis tool. Indeed the identification of these parameters is made possible by analysing experiments where the heating source is modulated. Profile modulations give access to the heat pulse diffusivity $\chi_{hp} = \chi + \nabla T \partial\chi/\partial\nabla T$, and thereby provide a stringent test of transport models.

3.2. Similarity principle [15]

An important feature of turbulent transport is the existence of a similarity principle, which states that 3 dimensionless parameters, among many others, play a central role [16,17]. These are the normalised gyroradius $\rho^* = \rho_s/a$ (a is

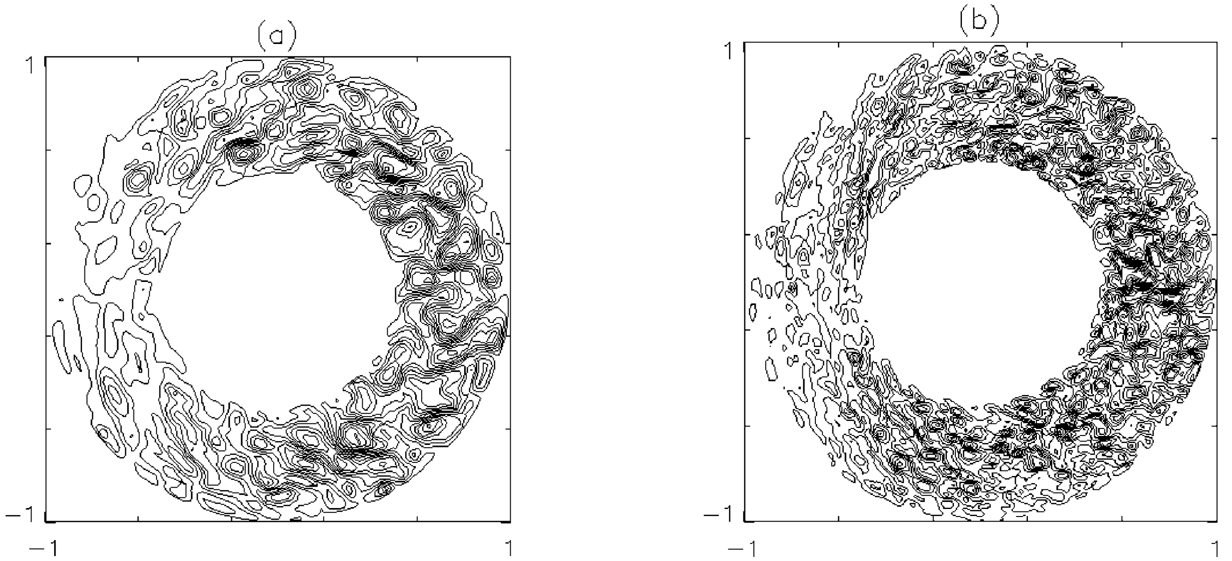

Fig. 5. Contour lines of the electric potential calculated with 3D full torus simulations of ion turbulence for two values of the normalised gyroradius $\rho^* = 1/50$ (a) and $\rho^* = 1/100$ (b) [19]. The size of the vortices is proportional to ρ^*. This behaviour is consistent with a gyroBohm scaling law.

the minor radius), collisionality $\nu^* = \nu_{ei} q R/\varepsilon_a^{3/2} v_{Te}$ (ν_{ei} the electron–ion collision frequency, $\varepsilon_a = a/R$ the inverse aspect ratio, v_{Te} is the thermal electron velocity) and plasma beta β.

Turbulence simulations indicate that the scaling law is 'gyroBohm' for small enough values of ρ^*. This means that correlation lengths, correlation times and diffusivity scale respectively as ρ_s, R/v_{Ts} and $\rho^* T_s/eB$ (v_{Ts} is ion thermal speed $(T_s/m_s)^{1/2}$), i.e.,

$$\chi_{gB} \equiv \frac{T_s}{eB}\rho^* \tag{7}$$

Since early 3D fluid simulations of ion turbulence [18,19], and more recent gyrokinetic simulations [20,21], it is now widely admitted that the correlation length and time, and the heat flux follow the gyroBohm prediction in the limit of small values of ρ^* (see Fig. 5 for an example). A departure from gyroBohm scaling is observed for a value of ρ^* above a critical value of ρ^*. The transport is then Bohm-like, i.e., the diffusion coefficient scales as T/eB. There is no consensus on the value of this critical normalised gyroradius and on the reason why the gyroBohm scaling is broken above this critical value.

The situation is less clear for β and collisionality parameters, because of competing effects. Collisionality has a stabilising effect on electron (TEM) modes due to electron collisional detrapping [22]. On the other hand, collisional friction damps zonal flows [23], which are fluctuations of poloidal velocity that reduce turbulent transport (see Section 5).

The dependence on β is mainly a signature of electromagnetic effects, and is also involved in the compression of magnetic surfaces (the Shafranov shift, which is stabilising, see Section 4). In collisionless plasmas, increasing β stabilises ITG/TEM modes. Above a critical value of β (kinetic) ballooning modes become unstable [3]. Turbulence simulations basically confirm this behaviour, i.e., a mild decrease of transport with increasing β, followed by a sharp increase of the diffusion coefficient above a critical value of β, of the order of half the ideal MHD β limit [24].

4. Turbulence control and transport barriers [25–27]

The physics of transport barriers is a broad subject that is already covered by several overview papers for external [28,29] and internal transport barriers [30,31]. Two generic key parameters are known to play a central stabilising role: flow shear and magnetic shear. Other ingredients may be involved (density gradient, ratio of electron to ion temperature, impurity content, ...), but are less generic than flow and magnetic shears.

4.1. Shear flow stabilisation

The physics of turbulent transport reduction due to $E \times B$ shear flow is well documented. The interested reader may consult overviews on theory [32] and experiments related to shear flow stabilisation [33]. Stabilisation results essentially from the shearing of turbulent convective cells. An approximate criterion for stabilisation is $\gamma_E > \gamma_{\rm lin}$ [34], where γ_E is the flow shear rate defined as (in a simplified geometry)

$$\gamma_E = \frac{\mathrm{d}}{\mathrm{d}r}\left(\frac{E_r}{B}\right) \tag{8}$$

and $\gamma_{\rm lin}$ is the maximum linear growth rate. Here B is the magnetic field and E_r is the radial electric field. A second criterion [35] consists in comparing a phase decorrelation time (Dupree time) to a turbulence correlation time

$$\left[k_\theta^2 \gamma_E^2 \mathrm{D}\right]^{1/3} \tau_c > 1 \tag{9}$$

where D is a diffusion coefficient and τ_c a turbulence auto-correlation time. The latter criterion requires measurements of D and τ_c, and is therefore more difficult to assess. Both criterions (8) and (9) are equivalent when using a mixing-length estimate for the diffusion coefficient and assuming $\gamma_{\rm lin}\tau_c = 1$. The radial electric field is constrained by the ion force balance equation

$$E_r = \frac{T_i}{e_i}\frac{\mathrm{d}n_i}{n_i\,\mathrm{d}r} + (1 - k_{\rm neo})\frac{\mathrm{d}T_i}{e_i\,\mathrm{d}r} + V_\varphi B_\theta \tag{10}$$

where the number $k_{\rm neo}$ depends on the collisionality regime and V_φ is the ion toroidal velocity. Once a barrier is formed, a positive loop takes place where density and ion temperature gradients increase, thus boosting the velocity shear rate. The situation is different at the onset of the barrier. The torque will be small in a reactor, so that $V_\varphi \approx 0$. Since typical growth rates are of the order of c_s/a, it is found that the ratio $\gamma_E/\gamma_{\rm lin}$ scales as the normalised gyro-radius ρ^*. This ratio is small in present tokamaks and will be even smaller in next step devices. This smallness is compensated in the edge by small values of the gradients length, which lead to a shear flow sufficient to trigger an external transport barrier above a critical value of the heat flux. The mechanisms at play are not entirely known to date. The situation is more complex for internal transport barriers. In this case, shear flow is usually not large enough by itself to trigger a barrier, and another mechanism is needed to lower the linear growth rate. Optimising the magnetic configuration, for instance by modifying the magnetic shear, provides a means to do this.

4.2. Negative magnetic shear and α stabilisation

Negative magnetic shear is known to decrease the interchange drive [36]. This effect is enhanced by the Shafranov shift of magnetic surfaces (also called α effect, $\alpha = -q^2 R\,\mathrm{d}\beta/\mathrm{d}r$ is a measure of the Shafranov shift) [37,38]. In fact this physics is related to the stability of MHD modes [39,40] and the 'access to second stability' (see for instance [41]).

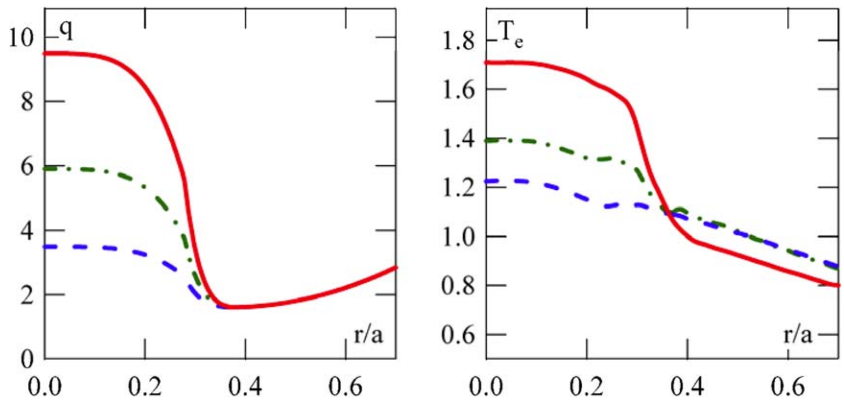

Fig. 6. Profiles of safety factor, and electron temperature calculated with the TRB turbulence code [42].

For electron modes, stabilisation occurs when $s < -3/8$, consistently with Eq. (1), while for ions the exact value depends on the poloidal structure of modes. This stabilisation scheme has been tested both with fluid and kinetic simulations. An electron transport barrier appears when the magnetic shear is negative, as shown on Fig. 6 [42]. This effect is amplified for values of α of the order of unity. For electron modes, theory predicts stability when $s < 3\alpha/5 - 3/8$. A similar effect exists for ions, which comes from the shear dependence of the ion curvature averaged over the mode structure $\lambda_i = \langle \cos(\theta) + (s\theta - \alpha \sin(\theta)) \sin(\theta) \rangle$. However, it is important to note that slab ITG modes are not sensitive to these effects, and remain unstable at negative magnetic shear. The resulting turbulence is nevertheless weaker.

5. Turbulence self-organisation [43,44]

Plasma turbulence self-organises through the formation of (large scale) structures, which back-react on (small scale) fluctuations. Two types of structures play a crucial role: zonal flows, which are fluctuations of the poloidal velocity, and large scale transport events. These are rare but efficient events in terms of turbulent transport, as they trigger relaxations of the mean profiles. Structure dynamics leads to turbulence intermittency, which makes difficult the use of statistical theories, often based on an assumption of Gaussian (or near Gaussian) statistics. Hence intermittency can be considered as the main reason why the predictive capability of the transport models based on a mixing-length assumption is limited.

5.1. Zonal flows

Zonal flows play an important role in turbulence simulations. It was found that computations with radial modes ($k_\theta = 0$, $k_\varphi = 0$) of the electric potential are characterised by a transport lower than in simulations where these modes are artificially suppressed [45,46]. The mechanism which is often advocated for the generation of zonal flows is the Reynolds stress $\langle \boldsymbol{v}_E \boldsymbol{v}_E \rangle$, whose non zero divergence drives the plasma velocity in poloidal and toroidal directions [23]. Another source of flow comes from flow compressibility (related to magnetic field curvature). Zonal flows back reacts on fluctuations provided that their frequency is small compared to turbulence frequencies. Stabilisation occurs via a process similar to the vortex shearing associated to a mean shear flow [23].

5.2. Large scale transport events

Several turbulence simulations exhibit large scale transport events, which enhance the anomalous transport. Two mechanisms have been identified: avalanches and streamers. Avalanches appear via a domino effect: if a gradient of temperature (or density) locally exceeds an instability threshold, it generates a burst of transport that expels some heat or matter, thus increasing the gradient on a neighbouring radial position, where the same process may occur again [47]. Streamers are convective cells that are elongated in the radial direction. They have been observed in particular in various turbulence simulations [48–50].

6. Fluctuation measurements [51]

Several diagnostics have been developed to measure fluctuations in tokamak plasmas. The most commonly used diagnostics are Langmuir probes, coherent laser scattering, reflectometers, heavy ion beam probe (HIBP), and Beam Emission Spectroscopy. Most of these measure density fluctuations. Langmuir probes and HIPB are also able to measure potential fluctuations and therefore give an estimate of particle fluxes. The role of these diagnostics has been crucial in the past to demonstrate that turbulence is responsible for transport in tokamaks. In particular it was proved that in edge plasmas, turbulence particle and energy fluxes agree with the fluxes deduced from particle and heat balance (i.e., integral of the particle and heating sources) [52]. Since then, several studies have confirmed the close connection between turbulence and transport. In particular, a reduction of the fluctuation level is observed when a transport barrier is formed [53]. In plasmas where the flow shear rate is high, a reduction of the correlation length is measured, consistently with theoretical expectation.

Turbulence diagnostics have also brought information on scaling laws [54]. It has been shown that the correlation lengths follow the gyroBohm expectation, i.e., are proportional to an ion Larmor radius. There is also a strong evidence that the large scale fluctuations play a prominent role as the perpendicular wave number spectrum is found to decrease as $k_\perp^{-3}$ for $k_\perp \rho_i < 1$, and even faster for $k_\perp \rho_i > 1$. Several pending issues remain, however. The reason why a gyroBohm scaling law is not always observed for the global confinement whereas the correlation lengths are always proportional to the gyroradius is still not understood. Also the scaling of fluctuations with collisionality and plasma β is not well known. This is presently a very active subject of research.

Turbulence intermittency is another important issue, which was discovered in edge plasmas with Langmuir probe measurements [55,56]. As mentioned previously, intermittency restricts the validity domain of transport models, which are often based on a Gaussian statistics assumption. Most of the effort is now devoted to the understanding of the spatio-temporal properties of fluctuations and their link with transport. One challenge is to prove the existence of zonal flows and large scale transport events. Indeed the underlying structures are believed to be responsible for turbulence intermittency. Zonal flows were detected in an unambiguous way with HIPB measurements [57]. To date, avalanches or streamers have not been directly observed. However, avalanche-like processes were observed on electron temperature profiles [58].

7. Conclusions

Although many aspects of turbulent transport in fusion plasmas are now understood, several challenges still stand ahead. First, a fully predictive transport model does not exist yet although impressive progress has been made in this direction. It is likely that the mixing-length estimate, which is the main recipe that underlies most transport models, needs to be modified in order to account for recent advances in the understanding of turbulence dynamics. Second, the ingredients leading to the formation and sustainment of transport barriers are not fully understood. It is clear that magnetic and flow shears are the main players that control transport barriers. However, the conditions for their development remain unclear. This is particularly true for the flow shear in external transport barriers. Clearly some progress is needed, as transport barriers are mandatory to design reactors with a reasonable size. Finally turbulence dynamics still resists the impressive amount of studies and investigations done up to now. One difficulty is now identified as the complex behaviour of structures, which are responsible for intermittency. Turbulence simulations and fluctuation measurements have brought an invaluable input in this matter and progress is made every day. However, gyrokinetic, i.e., 5D simulations are a formidable challenge in terms of computing resources, and also data analysis. Ultimately understanding the dynamics of turbulence should lead to a better control of transport. Control techniques based on the fine tuning of the magnetic configuration and flow shear in real-time are currently used in fusion devices. Whether more refined techniques can be used to control turbulence remains an open and challenging question.

References

[1] W. Horton, Rev. Mod. Phys. 71 (1999) 735.
[2] J. Weiland, Collective Modes in Inhomogeneous Plasmas, IOP, 2000.
[3] G. Rewoldt, W.M. Tang, R.J. Hastie, Phys. Fluids 30 (1987) 807.
[4] F. Jenko, W. Dorland, M. Kotschenreuther, B.N. Rogers, Phys. Plasmas 7 (2000) 1904.
[5] Y. Idomura, T.H. Watanabe, H. Sugama, Kinetic simulations of turbulent fusion plasmas, C. R. Physique 7 (2006), this issue.
[6] A.G. Peeters, C. Angioni, G. Tardini, Transport modelling, C. R. Physique 7 (2006), this issue.
[7] P. Mantica, F. Ryter, Perturbative studies of turbulent transport in fusion plasmas, C. R. Physique 7 (2006), this issue.
[8] H. Nordman, J. Weiland, A. Jarmen, Nucl. Fusion 30 (1990) 983.
[9] R.E. Waltz, G.M. Staebler, W. Dorland, et al., Phys. Plasmas 4 (1997) 2482.
[10] M. Kotschenreuther, W. Dorland, M.A. Beer, et al., Phys. Plasmas 2 (1995) 2381.
[11] C. Bourdelle, et al., Nucl. Fusion 42 (2002) 892.
[12] M. Erba, et al., Plasma Phys. Control. Fusion 39 (1997) 261.
[13] B. Coppi, N. Sharky, Nucl. Fusion 21 (1981) 1363.
[14] F. Imbeaux, F. Ryter, X. Garbet, Plasma Phys. Control. Fusion 43 (2001) 1503.
[15] D.C. McDonald, The dimensionless scaling of ELMy H-mode confinement, C. R. Physique 7 (2006), this issue.
[16] B.B. Kadomtsev, Sov. J. Plasma Phys. 1 (1975) 295.
[17] J.W. Connor, J.B. Taylor, Nucl. Fusion 17 (1977) 1047.
[18] X. Garbet, R.E. Waltz, Phys. Plasmas 3 (1996) 1898.
[19] M. Ottaviani, G. Manfredi, Phys. Plasmas 6 (1999) 3267.
[20] Z. Lin, S. Ethier, T.S. Hahm, W.M. Tang, Phys. Rev. Lett. 88 (2002) 195004.
[21] J. Candy, R.E. Waltz, Phys. Rev. Lett. 91 (2003) 045001.
[22] B.B. Kadomtsev, O.P. Pogutse, in: M.A. Leontovitch (Ed.), Reviews of Plasma Physics, vol. 5, Consultant Bureau, New York, 1970, p. 249.
[23] P.H. Diamond, et al., Plasma Phys. Control. Fusion 47 (2005) R35.

[24] P.B. Snyder, G.W. Hammett, Phys. Plasmas 8 (2001) 744.
[25] P. Gohil, Edge transport barriers in magnetic fusion plasmas, C. R. Physique 7 (2006), this issue.
[26] T. Tala, X. Garbet, JET EFDA contributors, Physics of Internal Transport Barriers, C. R. Physique 7 (2006), this issue.
[27] U. Stroth, M. Ramisch, Towards turbulence control in magnetised plasmas, C. R. Physique 7 (2006), this issue.
[28] K.H. Burrell, Plasma Phys. Control. Fusion 36 (1994) A291.
[29] ASDEX Team, Nucl. Fusion 29 (1989) 11.
[30] R.C. Wolf, Plasma Phys. Control. Fusion 45 (2003) R1.
[31] J.W. Connor, T. Fukuda, X. Garbet, et al., Nucl. Fusion 44 (2004) R1.
[32] P.W. Terry, Rev. Mod. Phys. 72 (2000) 109.
[33] K.H. Burrell, Phys. Plasmas 6 (1999) 4418.
[34] R.E. Waltz, G.D. Kerbel, J. Milovitch, Phys. Plasmas 1 (1994) 2229.
[35] H. Biglari, P.H. Diamond, P.W. Terry, Phys. Fluids B 2 (1990) 1.
[36] J.F. Drake, Y.T. Lau, P.N. Guzdar, et al., Phys. Rev. Lett. 77 (1996) 494.
[37] M. Beer, G.W. Hammett, G. Rewoldt, et al., Phys. Plasmas 4 (1997) 1792.
[38] C. Bourdelle, W. Dorland, X. Garbet, et al., Phys. Plasmas 10 (2003) 2881.
[39] J.W. Connor, R.J. Hastie, J.B. Taylor, Phys. Rev. Lett. 40 (1978) 396.
[40] J.F. Drake, et al., Phys. Rev. Lett. 77 (1996) 494.
[41] B. Coppi, A. Ferreira, J.-W.-K. Mark, J.J. Ramos, Nucl. Fusion 19 (1979) 715.
[42] Y. Baranov, et al., Plasma Physics Control. Fusion 46 (2004) 1181.
[43] C. Hidalgo, B.Ph. van Milligen, M. Angeles Pedrosa, Intermittency and structures in edge plasma turbulence, C. R. Physique 7 (2006), this issue.
[44] S. Benkadda, Open issues and trends in turbulent transport, C. R. Physique 7 (2006), this issue.
[45] M.A. Beer, Ph.D. thesis, Princeton University, 1995.
[46] Z. Lin, et al., Science 281 (1998) 1835.
[47] P.H. Diamond, T.S. Hahm, Phys. Plasmas 2 (1995) 3640.
[48] J.F. Drake, P.N. Guzdar, A.B. Hassam, Phys. Rev. Lett. 61 (1988) 2205.
[49] F. Jenko, W. Dorland, M. Kotschenreuther, B.N. Rogers, Phys. Plasmas 7 (2000) 1904.
[50] P. Beyer, S. Benkadda, X. Garbet, P.H. Diamond, Phys. Rev. Lett. 85 (2000) 4892.
[51] P. Hennequin, Scaling laws of density fluctuations in tokamak plasmas, C. R. Physique 7 (2006), this issue.
[52] Ch.P. Ritz, et al., Phys. Rev. Lett. 62 (1989) 1844.
[53] E. Mazzucato, et al., Phys. Rev. Lett. 77 (1996) 3145.
[54] P. Hennequin, et al., Plasma Phys. Control. Fusion 46 (2004) B121.
[55] R. Jha, et al., Phys. Rev. Lett. 69 (1992) 1375.
[56] B.Ph. van Milligen, C. Hidalgo, E. Sánchez, Phys. Rev. Lett. 74 (1995) 395.
[57] A. Fujisawa, et al., Phys. Rev. Lett. 93 (2004) 165002.
[58] P.A. Politzer, Phys. Rev. Lett. 84 (2000) 1192.